With best regards, Susanne

PROCEEDINGS OF THE INTERNATIONAL CONFERENCE

NONLINEAR SUPERCONDUCTING DEVICES AND HIGH-T$_c$ MATERIALS

Capri, Italy   8–13 October 1994

Editors

R D Parmentier
(University of Salerno, Italy)

N F Pedersen
(Technical University of Denmark)

World Scientific
Singapore • New Jersey • London • Hong Kong

NOVEL VORTEX DYNAMICS IN TWO-DIMENSIONAL JOSEPHSON ARRAYS[*]

SUSANNE G. LACHENMANN, T. DODERER, and R.P. HUEBENER
*Lehrstuhl für Experimentalphysik II, Universität Tübingen, Auf der Morgenstelle 14
D-72076 Tübingen, Germany*

and

P.A.A. BOOI and S.P. BENZ
National Institute of Standards and Technology, 325 Broadway, Boulder, CO 80303, U.S.A

ABSTRACT

We present spatially resolved studies of vortex dynamics in two-dimensional Josephson-junction arrays. For bias currents smaller than the array critical current, a small local thermal perturbation at the array boundaries lowers the vortex entry barrier and the array switches to the resistive state. For bias currents slightly above the array critical current, vortices and antivortices are nucleated at opposite edges of the array. An alternating crossing vortex motion is observed experimentally.

1. Introduction

In two-dimensional (2D) Josephson-junction arrays, vortices play a central role for the static and dynamic properties.[1] In the static case, several vortex configurations, depending on a perpendicular applied magnetic field are discussed in the literature. For a direct observation of these configurations, spatially resolved measurements are necessary. Runge and Pannetier[2] used magnetic decoration, where small particles of a magnetic material are deposited on the sample, yielding an image of the local magnetic field variation. Hallen et al.[3] used scanning Hall probes and Vu et al.[4] used scanning SQUID microscopy. Both methods directly measure the local magnetic fields of the vortices. Depending on the applied magnetic field, regions of periodically arranged vortices seperated by domain walls are observed.[2,3,4] In Refs. [5,6], we have reported on imaging results of the vortex dynamics in 2D arrays. We have discussed the vortex dynamics in 2D arrays in close analogy to the dynamics of Abrikosov vortices in the current-induced resistive state of thin-film type-II superconductors.[7,8]

2. Experimental Procedures

2.1. Samples

Figure 1 shows a typical array geometry. The arrays consist of square networks

Report Documentation Page

Public reporting burden for the collection of information is estimated to average 1 hour per response, including the time for reviewing instructions, searching existing data sources, gathering and maintaining the data needed, and completing and reviewing the collection of information. Send comments regarding this burden estimate or any other aspect of this collection of information, including suggestions for reducing this burden, to Washington Headquarters Services, Directorate for Information Operations and Reports, 1215 Jefferson Davis Highway, Suite 1204, Arlington VA 22202-4302. Respondents should be aware that notwithstanding any other provision of law, no person shall be subject to a penalty for failing to comply with a collection of information if it does not display a currently valid OMB control number.

1. REPORT DATE	2. REPORT TYPE	3. DATES COVERED
OCT 1994		**00-00-1994 to 00-00-1994**

4. TITLE AND SUBTITLE	5a. CONTRACT NUMBER
Novel Vortex Dynamics in Two-Dimensional Josephson Arrays	5b. GRANT NUMBER
	5c. PROGRAM ELEMENT NUMBER
6. AUTHOR(S)	5d. PROJECT NUMBER
	5e. TASK NUMBER
	5f. WORK UNIT NUMBER
7. PERFORMING ORGANIZATION NAME(S) AND ADDRESS(ES) **National Institute of Standards and Technology,525 Broadway,Boulder,CO,80303**	8. PERFORMING ORGANIZATION REPORT NUMBER
9. SPONSORING/MONITORING AGENCY NAME(S) AND ADDRESS(ES)	10. SPONSOR/MONITOR'S ACRONYM(S)
	11. SPONSOR/MONITOR'S REPORT NUMBER(S)

12. DISTRIBUTION/AVAILABILITY STATEMENT
Approved for public release; distribution unlimited

13. SUPPLEMENTARY NOTES
U.S. Government or Federal Rights License

14. ABSTRACT
see report

15. SUBJECT TERMS

16. SECURITY CLASSIFICATION OF:			17. LIMITATION OF ABSTRACT	18. NUMBER OF PAGES	19a. NAME OF RESPONSIBLE PERSON
a. REPORT **unclassified**	b. ABSTRACT **unclassified**	c. THIS PAGE **unclassified**	**Same as Report (SAR)**	**5**	

of superconducting wires (Nb and PbInAu) with Josephson junctions placed between the line crossings. The $Nb/AlO_x/Nb$ junctions (area $\approx 5~\mu m \times 5~\mu m$) have critical currents on the order of $i_c = 150~\mu A$. Typically, the 1σ-spread in i_c is less than 3 %.[9,10] Each of the junctions is externally shunted with an InAu resistor R_s of about 1.5 Ω, so the McCumber parameter is $\beta_{c,j} = 2\pi i_c R_s{}^2 C/\Phi_0 < 0.7$;[9] $\Phi_0 = h/2e$ is the flux quantum. The Josephson coupling energy $E_J = \hbar i_c/2e$ is about $E_J \approx 10^{-20} J$ and is 5 to 6 orders of magnitude larger than the charging energy $E_C = e^2/(2~C)$ (C is the junction capacitance). Hence, we deal with the classical limit, where charging effects can be neglected.[11] The bias current is fed to each of the array columns through InAu feeding resistors (not shown in Fig. 1) of about 0.5 Ω each. In 2D superconducting
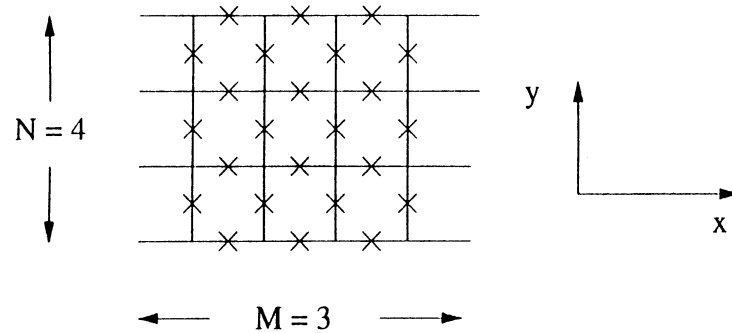

Fig. 1. Sketch of a typical array geometry with N columns of M junctions. The arrays consist of square networks of superconducting wires with Josephson junctions placed between the line crossings. Each junction is symbolized by a cross. The notation of the x and y direction is shown. The dc-bias current flows along the x-axis. The array voltage drop along the whole array is measured in the same direction.

arrays, flux quantization has to be taken into account so that the total sum of the junction phase differences ϕ around a loop is related to the flux Φ passing through the loop by

$$\sum_{loop} \phi = -2\pi \frac{\Phi}{\Phi_0} + 2\pi n, \qquad (1)$$

where n is an integer. There are two contributions to Φ: $\Phi = \Phi^{ext} + \Phi^{ind}_{i,j}$, where Φ^{ext} is due to an external magnetic field perpendicular to the array, and $\Phi^{ind}_{i,j}$ is the self-induced flux through the cell (i, j) due to the currents in the array.[12] The frustration $f = Ba^2/\Phi_0$ is defined as the normalized applied flux per unit cell. B is the externally applied magnetic field. The size of the square array unit cell is $a \approx 16.7~\mu m$. The electromagnetic radius of the vortex is given by the magnetic penetration depth

$$\lambda_\perp = \Phi_0/(2\pi\mu_0 i_c), \qquad (2)$$

where μ_0 is the permeability of the free space.[13] For our arrays, $\lambda_\perp < a$.

2.2. Electron beam imaging

Low temperature scanning electron microscopy (LTSEM) enables the spatially resolved investigation of superconducting devices and circuits during their operation at liquid helium temperatures. The basic principles are described in Ref.[14]. The essential points are the following: the sample film (on top of the substrate) is directly irradiated with an electron beam. The bottom side of the substrate is in contact with a liquid helium bath, thereby ensuring effective sample cooling. The temperature T of the sample is about 5 K. The electron beam focused at the coordinates (x_0, y_0) on the sample surface acts as a local heat source. The lateral dimension of the thermally perturbed area near (x_0, y_0) determines the spatial resolution of our images. This resolution is estimated to be about 3 μm for the samples used in the present studies. Typical values for the beam voltage and current are 25 kV and 100 pA, respectively, yielding a local temperature increment of about 1 K.

The difference of the time scales of the array dynamics and of the scanning procedure is important. The junction oscillation period is on the order of 10 ps, whereas the decay time of the beam-induced thermal perturbation is about 100 ns.[14] During scanning, the electron beam typically stays 3 ms at each position. Hence, the measured sample response to the beam irradiation represents time-averaged information on the time scale of the Josephson dynamics.

The sample is shielded from dc and ac magnetic fields by means of μ-metal screens at both room and liquid-helium temperature. Measuring the critical current as a function of the externally applied magnetic field B, we estimated the residual magnetic field to be smaller than 700 nT. This value corresponds to a frustration $f < 1/10$. During our measurements, the electron beam is scanned across the current-biased array. The beam is chopped at a frequency of 20 kHz, and the change in array voltage $\Delta V(x_0, y_0)$ induced by the beam is phase-sensitively recorded using a lock-in technique. Near the beam focus, the junction is heated from about 5 K to 6 K, which reduces the junction critical current i_c by about 20%. In these experiments, the local heating induces an array voltage signal $\Delta V(x_0, y_0) < 10\mu V$.

3. Experimental Results and Discussion

In this section we present results of our spatially resolved investigations on two-dimensional Josephson-junction arrays.
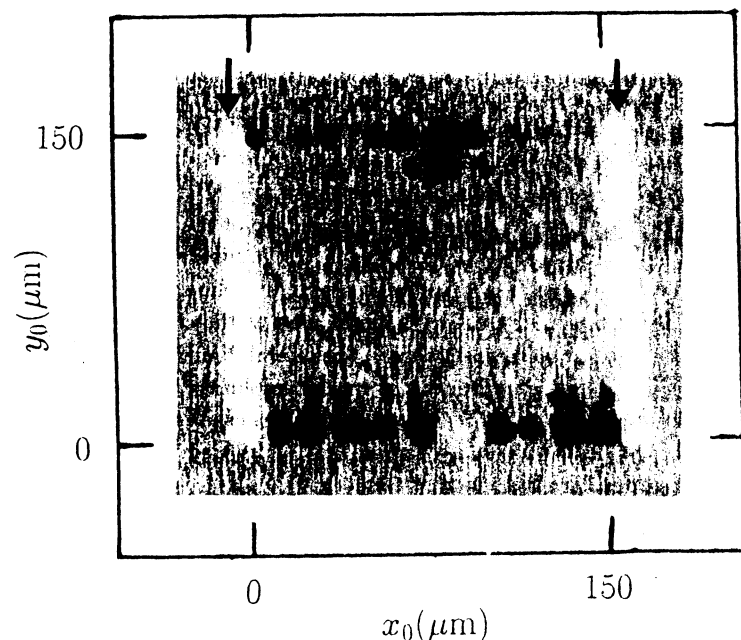
Fig. 2. Gray value representation of the voltage image $\Delta V(x_0, y_0)$ of a 10 × 10 array without groundplane at $T \approx 5K$. The array is biased at $I_b \approx 0.9 I_c$. The dc bias current flows horizontally through the array. The array boundaries lie between 0 μm and 150 μm in both directions. A positive (negative) electron beam induced voltage signal $\Delta V(x_0, y_0)$ is indicated by the dark (bright) areas, whereas $\Delta V(x_0, y_0) \approx 0$ is shown by the area surrounding the array. The signal level $|\Delta V|$ is about 100 nV. The rows of the feeding resistors are marked by arrows.

3.1. The Subcritical Region: $I_b < I_c$

First, we report on measurements where the bias current I_b was chosen smaller than the critical current I_c of the array.

Figure 2 shows the voltage image $\Delta V(x_0, y_0)$ for a 10×10 array. The array is biased at $I_b \approx 0.9$ mA. The array critical current is $I_c \approx 1$ mA. Since $I_b < I_c$, the sample is in the zero-voltage state without e-beam irradiation. In Fig. 2, a positive (negative) signal $\Delta V(x_0, y_0)$ is indicated by the dark (bright) areas, whereas the zero signal is shown by the gray level in the area surrounding the array.

Figure 2 is explained by edge nucleation of vortices induced by the self-field of the array's dc-bias current. The array's self-field is strongly peaked at the edges of the array (parallel to the bias current) and is antisymmetric with respect to the array center axis. Since for these studies $\lambda_\perp < a$, each magnetic flux quantum is confined
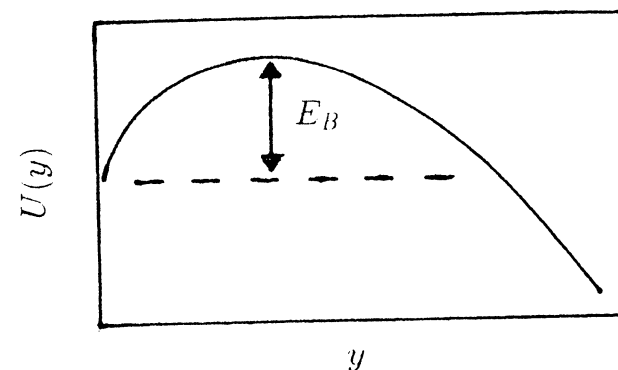

Fig. 3. Sketch of the energy $U(y)$ of a single vortex versus the y-coordinate for a bias current smaller than the array critical current.

to one unit cell. When the array is biased below I_c, the current-induced vortices are pinned at the array edges. One edge of the array supports vortices, the opposite side antivortices. The entrance barrier E_B, which prevents the vortices from entering the array, can be calculated from the Gibbs energy of a single vortex in the array.[5,15]

Figure 3 shows a sketch of the Gibbs energy $U(y)$ and E_B for bias currents smaller than the critical current. E_B is decreasing with increasing temperature T.

When the electron beam heats a junction at the edge of the array, E_B may be decreased below 0, and the vortices enter into the array. The vortices move perpendicular to the bias current and produce a voltage across the array. This process gives rise to voltage signals $+\Delta V(x_0, y_0)$ at each junction where vortices have formed and are depinned by the local heating due to the electron beam. From the spatial dependence of $\Delta V(y_0)$ we conclude that $\lambda_\perp < a$.

In Fig. 2, voltage signals $\Delta V < 0$ of about -5 nV are observed at the positions of the feeding resistors (marked by arrows). The resistance change $\Delta R = \Delta V/I_b$ is about -5 $\mu\Omega$. The origin of these signals is unclear.

Summarizing, for $I_b < I_c$, we observed electron-beam-induced vortex motion.

3.2. The Alternating Crossing Vortex Motion (ACVM)

Second, we report on measurements, where the bias current I_b was chosen slightly above the critical current.
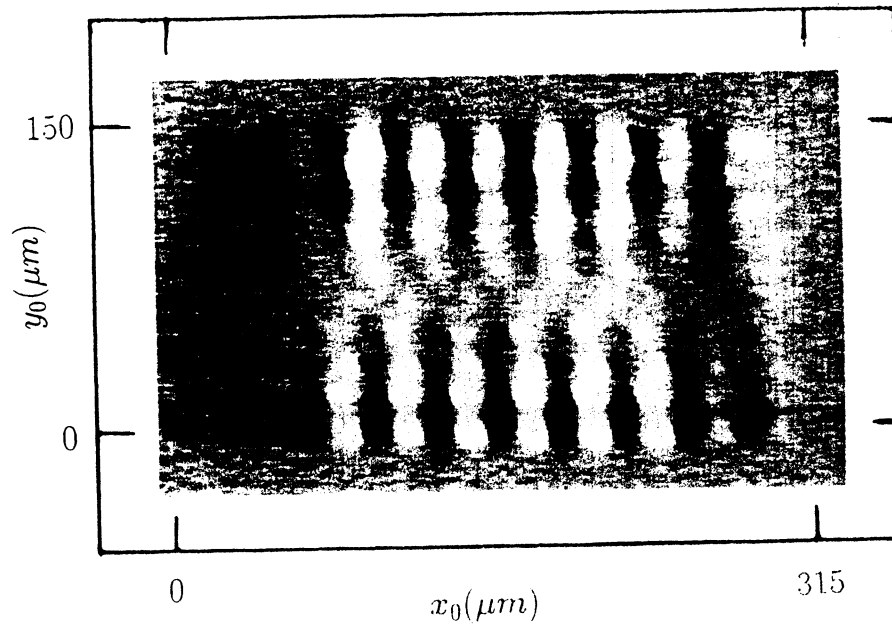
Fig. 4. Gray value representation of the voltage image $\Delta V(x_0, y_0)$ of a 20×10 array with a superconducting groundplane at $T \approx 5$ K. The array is biased at $I_b \approx 1.25$ mA and a corresponding voltage of 3 mV. The array critical current is $I_c \approx 750$ μA. The dc bias current flows horizontally through the array. The array boundaries lie between 0 μm and 150 μm in y-direction and between 0 μm and 315 μm in the x-direction. A positive (negative) electron beam induced signal $\Delta V(x_0, y_0)$ is indicated by the dark (bright) areas, whereas $\Delta V(x_0, y_0) \approx 0$ is shown by the gray value of the areas surrounding the array. The signal level $|\Delta V|$ is about 5 μV.

During their nucleation at the edges of the array, the vortices experience a Lorentz force perpendicular to the external current.

Figure 4 shows an imaging result for a 20×10 array. In simple terms, this can be explained as follows: when a vortex moves across a junction, this junction phase slips and the resulting voltage drop causes dissipation. When the electron beam is focussed at a junction where vortices are moving across, the vortex motion is changed due to the junction critical current reduction caused by the e-beam. No voltage signal is observed when the e-beam is focussed at a junction at which no vortices are crossing. The imaging thus resolves the vortex tracks. From a more detailed quantitative analysis of our imaging,[5] we calculate that the junctions where vortices enter the array give a positive voltage signal $\Delta V(x_0, y_0)$ (dark areas in Fig. 4). A negative

voltage change $\Delta V(x_0, y_0)$ (bright areas in Fig. 4) is measured at the positions where the vortices leave the array.

Inspection of Fig. 4 shows that for the bulk of the array, vortices are nucleated at the upper edge and anti-vortices at the lower edge of the array. They subsequently move through the array, perpendicular to the bias current, until they reach the opposite boundary, where they leave the array. Along the current direction there is a strong tendency to alternate between the direction of the vortex/antivortex motion. We call this behavior alternating crossing vortex motion (ACVM). Such alternation is favored due to the repulsion between vortices of the same vorticity and attraction between vortices of opposite vorticity.

For bias currents very close to, but larger than I_c, we did not observe the ACVM but an uncorrelated vortex motion. With increasing I_b the ACVM area grows, starting from the inner part of the array. Increasing I_b beyond the region where the ACVM is observed, the vortex density is increased and we observe a more complicated vortex motion. [6]

Recent numerical simulations based on the actual array parameters [16] have reproduced the ACVM.

Acknowledgments

References

[*] U.S. Government work not protected by U.S. copyright.

1. Conference volume Coherence in Superconducting Networks, Proceedings of the NATO Advanced Research Workshop, Delft, The Netherlands, 1987, [Physica B 152 (1987)]
2. K. Runge and B. Pannetier, Europhys. Lett. 24, 737 (1993)
3. H.D. Hallen, R. Seshadri, A.M. Chang, R.E. Miller, L.N. Pfeiffer, K.W. West, C.A. Murray, and H.F. Hess, Phys. Rev. Lett. 71, 3007 (1993)

4. L.N. Vu, M.S. Wistrom, D.J. Van Harlingen, Appl. Phys. Lett. **63**, 1693 (1993)

5. S. G. Lachenmann, T. Doderer, D. Hoffmann, R.P. Huebener, P.A.A. Booi, S.P. Benz, Phys. Rev. B **50**, 3158 (1994)

6. T. Doderer, S.G. Lachenmann, R.P. Huebener, P.A.A. Booi, S.P. Benz, to be published in IEEE Trans. Appl. Supercond.

7. R.P. Huebener, *Magnetic Flux Structures in Superconductors*, Springer-Verlag, Berlin, Heidelberg, New York (1979)

8. L.G. Aslamazov and A.I. Larkin, Sov.Phys.-JETP **41**, 381 (1975)

9. S. P. Benz and C. J. Burroughs, Appl. Phys. Lett. **58**, 2162 (1991)

10. S. P. Benz and C. J. Burroughs, Supercond. Sci. Technol. **4**, 561 (1991)

11. H.S.J. van der Zant, F.C. Fritschy, T.P. Orlando, and J.E. Mooij, Phys. Rev. B **47**, 295 (1993)

12. J.R. Phillips, H.S.J. van der Zant, J. White, and T.P. Orlando, Phys. Rev. B **47**, 5219 (1993)

13. K.K. Likharev, *Dynamics of Josephson junctions and circuits*, Gordon and Breach Science Publishers, New York (1986)

14. R.P. Huebener in: *Advances in Electronics and Electron Physics*, P.W. Hawkes, ed., Academic Press, New York, Vol. **70**, (1988), p. 1

15. H.S.J. van der Zant, H.A. Rijken, and J.E. Mooij, J. Low Temp. Phys. **79**, 289 (1990)

16. Th. Hagenaars, University of Utrecht, private communication (1994)

IN-SITU SPATIALLY RESOLVED INVESTIGATIONS
OF JOSEPHSON STRUCTURES WITH
A SCANNING LASER MICROSCOPE

J. HOLM AND J. MYGIND

Physics Department, Technical University of Denmark
DK-2800 Lyngby, Denmark

ABSTRACT

Most of the experimental studies of the static and dynamical states in Josephson junctions are limited to measuring the current-voltage characteristic under various experimental conditions, which, however, only provides a spatially averaged information on the processes inside the junction. We have therefore constructed a simple and reliable Cryogenic Scanning Laser Microscope for *in-situ* spatially resolved investigations of Josephson junctions. Usually the dynamical processes are very sensitive to external noise, making it essential for a microscope of this kind to have a very low noise level. This is met in combination with the demands for a high spatial resolution using a laser beam emitted from a 3.5 μm diameter optical fiber mounted on a piezoelectric scanner. Recent measurements on static and dynamical states of Josephson junctions are presented and discussed.

1. Introduction

Due to recent improvements in the fabrication of integrated superconducting circuits based on Josephson tunnel junctions it has become important to understand in detail the very complex dynamics on which their operation is based. For many years the only way to characterize the junctions has been to investigate their dc properties under various experimental conditions, like measuring the current-voltage (IV) characteristic and the critical current as function of magnetic field ($I_c(H)$). Such integral experiments do not provide direct spatially resolved information on the dynamics of this highly nonlinear device.

Several attempts have been made to overcome this. Already in 1983 Scheuermann et al.[1] designed the first scanning laser microscope consisting of two parts: (i) A room temperature optical setup with a helium-neon laser and focusing optics, and (ii) a standard optical cryostat with windows providing access for the laser beam to the sample which is positioned on a cold finger in the vacuum space. Josephson junctions with various geometries were investigated in the static state by measuring the reduction of the critical current caused by heating the junction with a 15-20 μm diameter laser spot[2].

Doderer et al.[3] utilized a conventional scanning electron microscope (SEM) in which the standard sample holder was replaced by a small liquid helium cryostat. The electron beam can be focused within a hundred nanometers so used as heating